

This is a repository copy of *Polyamines are required for normal growth in sinorhizobium meliloti*.

White Rose Research Online URL for this paper:

<https://eprints.whiterose.ac.uk/id/eprint/130198/>

Version: Accepted Version

Article:

Becerra-Rivera, Victor A., Bergström, Ed, Thomas-Oates, Jane orcid.org/0000-0001-8105-9423 et al. (1 more author) (2018) Polyamines are required for normal growth in *sinorhizobium meliloti*. Microbiology (Reading, England). 000615. pp. 600-613. ISSN: 1465-2080

<https://doi.org/10.1099/mic.0.000615>

Reuse

Items deposited in White Rose Research Online are protected by copyright, with all rights reserved unless indicated otherwise. They may be downloaded and/or printed for private study, or other acts as permitted by national copyright laws. The publisher or other rights holders may allow further reproduction and re-use of the full text version. This is indicated by the licence information on the White Rose Research Online record for the item.

Takedown

If you consider content in White Rose Research Online to be in breach of UK law, please notify us by emailing eprints@whiterose.ac.uk including the URL of the record and the reason for the withdrawal request.

Polyamines are required for normal growth in *Sinorhizobium meliloti*

Victor A. Becerra-Rivera¹, Ed Bergström², Jane Thomas-Oates² and Michael F. Dunn^{1*}

Author affiliations: ¹Programa de Genómica Funcional de Procariotes, Centro de Ciencias Genómicas, Universidad Nacional Autónoma de México, Cuernavaca, Morelos 62210, Mexico. ²Centre of Excellence in Mass Spectrometry and Department of Chemistry, University of York, Heslington, York, YO10 5DD, UK.

***Correspondence:** Michael F. Dunn, mike@ccg.unam.mx

Key words: *S. meliloti*; polyamines; putrescine; spermidine; homospermidine; norspermidine; ornithine decarboxylase

Abbreviations: ADC, arginine decarboxylase; Agm, agmatine; Arg, L-arginine; L-Asp β -SA, L-aspartate β -semialdehyde; Cad, cadaverine; Cb, carbenicillin; CID, collision induced dissociation; DAP, 1,3-diaminopropane; DNS, dansyl group; DNSCl, dansyl chloride; DNS-PA, dansyl-polyamine; FT-ICR, Fourier-transform ion cyclotron resonance; Gm, gentamicin; Gus, β -glucuronidase; *gusA*, gene encoding β -glucuronidase; HPTLC, high performance thin layer chromatography; HSpd, homospermidine; Km, kanamycin; LB, Luria-Bertani; Lys, L-lysine; LDC, lysine decarboxylase; MALDI, matrix-assisted laser desorption/ionisation; MMS, minimal medium succinate-ammonium; MMS-acid, MMS medium, pH 5.5; MMS-Salt, MMS medium with 0.3 M NaCl; MS, mass spectrometry; MS/MS, tandem mass spectrometry; μ , generations h^{-1} ; Nm neomycin; NSpd, norspermidine; OD₆₀₀, optical density at 600 nm; ODC, ornithine decarboxylase; *odc1*, gene encoding ornithine decarboxylase SMa0680; *odc2*, gene encoding lysine/ornithine decarboxylase SMc02983; Orn, L-ornithine; PA, polyamine; Put, putrescine; PY, peptone-yeast extract; Sp, spectinomycin; Spd, spermidine; Spm, spermine; Sm, streptomycin; TCA, trichloroacetic acid; TSS, transcriptional start site.

One supplementary table and one supplementary figure are available with the online Supplementary Material.

Subject category: Physiology and metabolism

Word count: 6,279

Abstract

Polyamines (PAs) are ubiquitous polycations derived from basic L-amino acids whose physiological roles are still being defined. Their biosynthesis and functions in nitrogen-fixing rhizobia such as *Sinorhizobium meliloti* have not been extensively investigated. Thin layer chromatographic and mass spectrometric analyses showed that *S. meliloti* Rm8530 produces the PAs putrescine (Put), spermidine (Spd) and homospermidine (HSpd) in their free forms and norspermidine (NSpd) in a form bound to macromolecules. The *S. meliloti* genome encodes two putative ornithine decarboxylases (ODC) for Put synthesis. Activity assays with the purified enzymes showed that ODC2 (SMc02983) decarboxylates both ornithine and lysine. ODC1 (SMa0680) decarboxylates only ornithine. An *odc1* mutant was similar to the wild type in ODC activity, PA production and growth. In comparison to the wild type, an *odc2* mutant had 45 % as much ODC activity and its growth rates were reduced by 42, 14 and 44 % under non-stress, salt stress or acid stress conditions, respectively. The *odc2* mutant produced only trace levels of Put, Spd and HSpd. Wild type phenotypes were restored when the mutant was grown in cultures supplemented with 1 mM Put or Spd or when the *odc2* gene was introduced *in trans*. *odc2* gene expression was increased under acid stress and reduced under salt stress and with exogenous Put or Spd. An *odc1 odc2* double mutant had phenotypes similar to the *odc2* mutant. These results indicate that ODC2 is the major enzyme for Put synthesis in *S. meliloti* and that PAs are required for normal growth *in vitro*.

INTRODUCTION

Polyamines (PAs) are low molecular weight organic compounds with two or more amino groups that are positively charged at neutral pH [1]. With few exceptions, PAs are ubiquitous in all organisms and have important roles in processes as diverse as growth, stress resistance and the regulation of transcription and translation in both eukaryotes and prokaryotes [2-5]. In contrast to their essential functions in eukaryotes and archaea, the physiological roles of PAs in bacteria are less clearly defined. In prokaryotes, PAs are involved in biofilm formation, stress

resistance, motility, pathogenesis, and growth. [6-12]. This diversity of functions might explain the presence of the more varied PA repertoire in bacteria [5].

Diamines found in bacteria include putrescine (Put), cadaverine (Cad) and 1,3-diaminopropane (DAP) (Fig. 1). Put is produced by nearly all bacteria, Cad is common in Proteobacteria and DAP is found sporadically in diverse phyla. Spermidine (Spd) is the most commonly found triamine, though bacteria may produce the related homospermidine (HSpd) and/or, less commonly, norspermidine (NSpd) [2,5,13].

Put can be made by the decarboxylation of L-ornithine (Orn) by Orn decarboxylase (ODC; EC 4.1.1.17) or of L-arginine (Arg) by Arg decarboxylase (ADC; EC 4.1.1.19). The ADC reaction produces agmatine (Agm), which is converted to Put by agmatinase (SpeB; EC 3.5.3.11). Cad is produced by lysine decarboxylase (LDC; EC 4.1.1.18) acting on L-lysine (Lys). Some decarboxylases have activity with both Lys and Orn as substrates [5,13,14].

In *Sinorhizobium meliloti* and other nitrogen-fixing rhizobia, work on PAs has focused on their identification and quantification during free-living growth [15,16], changes in their levels *in nodulo* when host plants were subjected to abiotic stress, or determining the effects of exogenous polyamines on symbiosis [12,17-21]. A few studies using biochemical and genetic approaches have shown species-dependent requirements for different PAs for growth, biofilm formation and motility in rhizobia [11,22-25].

Three studies with different strains of *S. meliloti* grown in minimal medium show that its free PA fraction invariably contains Put, Spd and HSpd, with Cad found in two of the studies [15,16,19]. Hamana et al. [16] assayed for, but did not detect, Agm, spermine (Spm), NSpd or DAP in *S. meliloti* IAM 12611. PAs in *S. meliloti* 1021 have been reported only for cultures grown in rich medium, where Put, Spd, HSpd and Spm were detected [19]; the latter probably originates from Spm present

in the tryptone and yeast extract components of the medium [14]. In contrast to other rhizobia, the genome sequence of strain 1021 indicates that it is able to synthesize NSpd, which has not been reported in rhizobia, and possesses an “alternative” pathway for Spd synthesis [14]. The strain 1021 genome encodes three putative basic amino acid decarboxylases. *sma0682* is annotated as a “decarboxylase (lysine, ornithine, arginine)” but its genomic context and sequence suggest that it encodes an ADC. We predicted that *sma0680* (annotated as “amino acid (ornithine, lysine, arginine) decarboxylase”) encodes an ODC: we denominate this gene and enzyme as *odc1* and ODC1, respectively. *smc02983* is annotated as an “ornithine, DAP, or arginine decarboxylase” but its product has sequence characteristics that suggest it is able to decarboxylate both lysine and ornithine [14,26]. We refer here to the *smc02983* gene and protein product as *odc2* and ODC2, respectively (Fig. 1).

Because *S. meliloti* has multiple enzymes catalyzing the conversion of *N*-acetylornithine to Orn during Arg biosynthesis [27] and is also able to produce Orn with an inducible arginase [14,26], we hypothesized that Orn is the major precursor for Put synthesis in this organism [27]. If this is correct, then ODC1 and/or ODC2 should be the key enzyme(s) for the synthesis of Put and the PAs derived from it (Fig. 1). The work presented here shows that ODC2 is responsible for synthesizing the majority of the Put produced by *S. meliloti* and that PAs are important for normal growth in minimal medium cultures with and without abiotic stress.

METHODS

Bacterial strains, plasmids and culture growth conditions

Bacterial strains and plasmids are listed in Table 1. PY and LB complex media, and MMS minimal medium with succinate and NH₄Cl as carbon and nitrogen sources, respectively, were described previously [27]. Salt stress was caused by growing cultures in MMS-salt medium, where NaCl was added to MMS to a final concentration of 0.3 M before adjusting the pH to 6.8 and autoclaving. For growth under acidic stress, MMS-acid medium was prepared by adjusting MMS medium to

pH 5.5 (rather than 6.8) before autoclaving. PA and amino acid supplements were prepared as 0.5 M stocks, adjusted to pH 6.8 (for use in MMS and MMS-salt) or pH 5.5 (for use in MMS-acid) and filter sterilized. To grow *S. meliloti* strains, cells from 3 day PY plates with appropriate antibiotics were used to inoculate 3 ml of liquid PY containing the same antibiotics and incubated at 200 rpm, 30°C. After 24 h, 1 ml of these cultures were used to inoculate 50 ml of PY containing one-half the normal concentration of antibiotics, in 125 ml baffled flasks. These cultures were incubated as above for 24 h, harvested by centrifugation at 5500 x g for 5 min, the cells washed twice in MMS and resuspended to an OD₆₀₀ of approximately 1.5 in MMS. These suspensions were used to inoculate the desired minimal medium without antibiotics to an initial OD₆₀₀ of 0.05: for transcriptional fusion and PA analyses, respectively, the medium:baffled flask volume ratios were 50:125 ml and 100:250 ml. Cultures were grown with agitation at 200 rpm at 30°C and growth was monitored at 600 nm. Specific growth rates (μ , generations h⁻¹) were calculated [28] from culture OD₆₀₀ values obtained between 4 and 12 h under non-stress conditions and 4 to 24 h under stress conditions. When required, antibiotics were used at the following concentrations (μ g ml⁻¹): carbenicillin (Cb), 50; gentamicin (Gm), 15; kanamycin (Km), 50; neomycin (Nm), 60; spectinomycin (Sp), 100; streptomycin (Sm), 200.

DNA manipulations

Standard protocols were used to grow *E. coli* and for DNA isolation, restriction digests, cloning and transformation [29]. Bacterial conjugations were performed as described previously [27]. High-stringency DNA hybridizations were done with a DIG-High Prime DNA Labeling kit (Roche).

PCR amplifications

DNA sequences were obtained from GenBank (www.ncbi.nlm.nih.gov/gene/). Primers (Table S1, Supplementary material) were used in PCR reactions with Accuprime Taq DNA polymerase (Invitrogen) to clone genes for the construction of transcriptional fusions or whose products were to be overexpressed and purified, or with Dream Taq PCR master mix (Thermo) for other purposes. PCR cycling programs included a denaturing step at 95°C for 1 min followed by 30 cycles of 95°C for 1 min, 56°C for 1 min and 72°C for a time appropriate for the length of the DNA being amplified. A final elongation step was made at 72°C for 10 min. For use in cloning, PCR products were purified with a commercially available kit.

Recombinant protein purification

S. meliloti genes *odc1* and *odc2* were amplified by PCR (Table S1) and cloned in pET Sumo to generate plasmids pSumo-*odc1* and pSumo-*odc2* (Table 1). These plasmids were used to overexpress the corresponding 6His-Sumo tagged protein products in *E. coli* BL21(DE3). For overexpression and purification, strain BL21(DE3) transformed with either pSumo-*odc1* or pSumo-*odc2* were grown in 100 ml LB Km at 37°C, 200 rpm to an OD₆₀₀ of 0.4, IPTG was added to a final concentration of 1 mM and incubation continued for 8 and 14 h, respectively. 6His-Sumo tagged proteins were purified using Ni-NTA resin (Invitrogen) under hybrid conditions following the manufacturer's protocol.

Mutant construction

Mutants of *S. meliloti* Rm8530 were constructed by the insertional inactivation of genes as described previously [27]. Briefly, genome regions encoding *odc1* and *odc2* were amplified by PCR (Table S1) and cloned into pCR 2.1-Topo to produce plasmids pCRodc1 and pCRodc2 (Table 1). Following verification by restriction enzyme analysis, the inserts from pCRodc1 and pCRodc2 were excised with *Sma*I/*Xba*I and *Sa*I, respectively, and inserted into suicide vector pK18mobsacB cut with *Sma*I/*Xba*I or *Xho*I to give plasmids pKodc1 and pKodc2 respectively. The loxP Sp cassette from pMS102loxSp17 was ligated into the *Bam*HI and *Sa*I sites

of the genes cloned in pKodc1 and pKodc2, respectively, generating plasmids pKodc1::loxSp and pKodc2::loxSp (Table 1). These constructs were introduced into *S. meliloti* Rm8530 by triparental mating using *E. coli* DH5 α /pRK2013 as helper. A Sp^r Nm^r single recombinant obtained from each mating was spread on PY containing Sm, Sp and 12 % sucrose to allow the selection of the 8530 *odc1* and 8530 *odc2* mutants (Table 1). The 8530 *odc1 odc2* double mutant was constructed in two steps. First, the loxP Sp interposon in the *odc1* gene in the 8530 *odc1* mutant was deleted by introducing plasmid pBBRMCre, which expresses the loxP-specific Cre recombinase, into the mutant. The desired loxP Sp deletion and pBBRMCre plasmid-cured strain was selected by screening for the Sm^r Sp^s and Sm^r Gm^s phenotypes, respectively [30]. In the second step, plasmid pKodc2::loxSp was introduced into the 8530 *odc1* loxSp-deleted mutant to obtain the 8530 *odc1 odc2* double mutant by selection for sucrose sensitivity. The correct construction of the mutants was confirmed by Southern hybridization.

Genetic complementation of the 8530 *odc2* mutant

To test genetic complementation of the *odc2* mutant, we excised the *Eco*RI fragment from pCRodc2, which contains the *odc2* gene with its native promoter and terminator regions, and introduced it into pBB5 to give plasmid pBB5-*odc2*. This plasmid, or pBB5 without an insert, was introduced into the 8530 *odc2* mutant by triparental mating.

Basic amino acid decarboxylase assays

The radiochemical assay for determining ODC activity in intact cells was modified from that of Romano et al. [31]. Cells from 16 h cultures were washed twice with 100 mM potassium phosphate buffer, pH 7 (KP 7) and resuspended to an OD₆₀₀ of 3.0. Assay mixtures (250 μ l) contained 100 mM KP 7, 4.5 mM MgSO₄, 3 mM β -mercaptoethanol and 85 nM pyridoxal-5'-phosphate. Individual reactions were started by adding L-ornithine to a final concentration of 3.5 mM containing 0.025 μ Ci of L-[1-¹⁴C]-ornithine. Assay mixtures were deposited in plastic tubes in which a CO₂ trap consisting of a 2 x 2.5 cm piece of filter paper wet with 125 μ l of 1 M

NaOH was placed so as to adhere to the top portion of the tube. Fifty μ l aliquots of cell suspension were added to the tubes, which were sealed with rubber septa and incubated for 4 h at 30°C. Reactions were stopped by adding 200 μ l of 10 % trichloroacetic acid (TCA) and samples were re-capped and left at room temperature for one hour. The paper CO₂ traps were mixed with 10 ml of Ultima Gold LSC cocktail (Sigma) and radioactivity determined by liquid scintillation counting. One unit (U) of activity is defined as the production of 1 nmol CO₂ min⁻¹ mg protein⁻¹. Total cellular protein was determined as described previously [32]. Decarboxylase activities of the purified 6His-Sumo-ODC1 or 6His-Sumo-ODC2 enzymes were determined using colorimetric assays with Arg [33], Orn [34] or Lys [35] as substrates. Assay of purified enzymes was done using 25-30 μ g of purified 6His-Sumo-ODC1 or 6His-Sumo-ODC2 per reaction and 1 U of activity is defined as the production of 1 nmol of decarboxylation product min⁻¹ mg protein⁻¹. Protein concentrations were determined by the Bradford method [36].

Construction of a *odc2* transcriptional fusion with the β -glucuronidase (*gusA*) gene

odc2 is the first gene of a predicted two gene operon but does not contain a predicted transcription start site (TSS) [37]. The PCR primers used to amplify the upstream and 5' coding region of *odc2* are described in Table S1, and the amplified region was cloned into pTZ57R/T (Table 1). The *gusA* fusion with this gene, plasmid pBB53odc2::*gusA*, was constructed using the PCR product of *odc2* that includes the 586 nt intergenic region between its start codon and that of the divergently transcribed *smc02984* gene, 19 and 297 nt of the of the *smc02984* and *odc2* coding regions, respectively. A clone containing the pTZ57R/T plasmid with the PCR product in the desired orientation was identified by digestion with appropriate restriction enzymes. The insert from the plasmid was excised with *Apal/XbaI* and cloned into vector pBBMCS-53 cut likewise, transcriptionally fusing the *odc2* promoter/5' region to the *gusA* gene. The correct transcriptional orientation of the fusion plasmid was confirmed by restriction enzyme digestion and in PCR reactions with primer p53lw (reverse primer specific for *gusA*) and the

forward primer for *odc2* (Table S1; [27]). The fusion plasmid was transferred to *S. meliloti* Rm8530 by triparental mating.

β-glucuronidase (Gus) assays

Experimental cultures were grown in the desired minimal medium for 16 h at 30°C with shaking at 200 rpm. Gus activity was determined by measuring the production of *p*-nitrophenol from the *p*-nitrophenyl β-D-glucuronide substrate with quantitation based on total protein [27]. One unit (U) of activity is defined as the production of 1 nmol of product min⁻¹ mg protein⁻¹. Strain Rm8530 containing pBBMCS-53 without an insert lacked Gus activity under the growth conditions tested.

Polyamine analysis by High Performance Thin-Layer Chromatography (HPTLC)

Dansyl (DNS) derivatives of PAs were analyzed by HPTLC using modifications of previously published protocols [38,39]. Cells from 32 h cultures were pelleted by centrifugation at 5500 x *g* for 5 min and resuspended to an OD₆₀₀ of 3.0 in fresh MMS. Cells from 1 ml portions of these suspensions were pelleted at 13,200 x *g*, resuspended with 0.5 ml of 5 % (w/v) TCA and stored at 4°C for 18-24 h. Free PAs present in the TCA supernatants, obtained by centrifugation at 13,200 x *g* for 10 min, were derivatized in 2 ml glass vials by mixing 40 µl of the supernatant, 80 µl of dansyl-chloride (DNSCI) solution (5 mg ml⁻¹ in acetone) and 40 µl of supersaturated aqueous sodium carbonate. Reaction mixtures containing PA standards (1.2 µg of the PA in 40 µl of 5 % TCA) were derivatized in the same way. The capped vials were heated at 80°C for 1 h, cooled to room temperature and quenched with 20 µl of L-proline solution (150 mg ml⁻¹ in water) for 30 min at room temperature in darkness. The reaction mixtures were extracted twice with 100 µl of toluene and the combined extracts dried under a stream of N₂. Samples of DNS-PA standards and DNS-PAs from cells were resuspended with 100 and 45 µl of toluene, respectively. One µl of DNS-PA standards or 10 µl of DNS-PAs from cells were run on Silica Gel 60 HPTLC plates (Merck) using chloroform/triethylamine (5:1 v/v) as mobile phase. For the routine determination of PAs produced by *S.*

meliloti cells from cultures, only the free PA fraction was analyzed. PAs can exist as free molecules in the cytoplasm or as forms bound to macromolecules such as proteins, lipids or nucleic acids. These bound forms of PAs can be obtained in their free forms by strong acid hydrolysis of the TCA-precipitated macromolecules [14]. We analyzed PAs bound to macromolecules as follows. Pellets of insoluble material obtained from treating cells with 5 % TCA were washed with 0.5 ml of 5 % TCA and the pellets resuspended with 0.5 ml of 6 N HCl. The suspensions were heated at 110°C for 18-24 h in 2 ml V-Vials with teflon-lined caps (Sigma). Twenty µl of hydrolysate was combined with 40 µl each of the DNSCI and supersaturated sodium carbonate solutions described above, and derivatization and HPTLC carried out as for free PAs. Plates were visualized under UV light and images captured with a Syngene (Frederick, MD, USA) InGenius imaging system. Densitometric quantification was done using ImageJ 1.48v software. For mass spectrometric analysis, the silica gel corresponding to DNS-PA spots were scraped off the TLC plates and eluted with methanol. After passage through 0.22 µM cellulose acetate filter units (Costar), methanol was removed under a N₂ stream. The samples were reconstituted in 200 µl acetonitrile:H₂O (1:1; v:v) containing 0.25% (v:v) formic acid.

Mass spectrometric analysis of dansyl-PAs

MALDI mass spectra were acquired using a Bruker 9.4T solariX XR Fourier-transform ion cyclotron resonance (FT-ICR) mass spectrometer (Bremen, Germany). The samples were ionized in positive ion mode using the MALDI ion source with α-cyano-4-hydroxycinnamic acid (CHCA) matrix. Sample spots were produced by premixing 1.4 µl of sample solution with the same volume of matrix solution (saturated solution in acetonitrile:H₂O (1:1; v:v) containing 0.25% (v:v) formic acid); 1 µl of this mixture was spotted onto a stainless steel target plate and allowed to air dry at ambient temperature. Spectra were measured with a transient length of 2.2 s resulting in a resolving power of 400000 at *m/z* 400. The instrument was externally calibrated using a standard peptide mix and a 'lock-mass' calibration was used with the matrix ion with *m/z* 568.135. Collision induced dissociation

(CID) was used to generate product ions and was achieved in the hexapole collision cell using argon as the collision gas. Product ion spectra were recorded with a transient length of 1.1 s, giving a resolution of 200000 at m/z 400.

RESULTS AND DISCUSSION

Identification of PAs produced by *S. meliloti* Rm8530

The work reported here uses *S. meliloti* Rm8530 as wild type. This strain is identical to the sequenced and well-characterized strain 1021 except that it has a functional copy of the *expR* gene, whose product is involved in quorum-sensing based transcriptional regulation [40]. PA production by strain Rm8530 has not been reported previously. By HPTLC analysis, we found no quantitative or qualitative differences in the PAs produced by strains 1021 and Rm8530 grown under the conditions reported here (results not shown).

Selected *S. meliloti* dansyl-PA (DNS-PA) derivatives and DNS-derivatives of authentic PA standards were isolated from HPTLC plates (Fig. S1 (a), Supplementary material) and analyzed by MALDI high resolution, high mass accuracy FT-ICR mass spectrometry (MS) and product ion tandem mass spectrometry (MS/MS). The details of this analysis are described in Fig. S1, Supplementary material. The reason for this analysis was to unambiguously identify DNS-PA spots present on our HPTLC plates, and this was particularly important for HSpd, for which no commercial standard is available, and for NSpd, which has not been reported in rhizobia.

As mentioned, PA analyses of various *S. meliloti* grown in culture showed the presence of Put, Spd, HSpd and (usually) Cad, but not Agm, spermine (Spm), NSpd or DAP. Our analysis of the PAs produced by strain Rm8530 grown in MMS (Fig. S1) shows the presence of Put, Spd, HSpd and NSpd, with the latter found only in the bound PA fraction. The presence of NSpd only in the bound fraction explains why it has not been detected previously in *S. meliloti*. Our results also indicate that Cad (or a Cad-like compound) is produced. We tentatively identified

DAP in cells from PA-supplemented cultures (described later), while neither Agm nor Spm were detected under any growth condition (results not shown).

Amino acids decarboxylated by ODC1 and ODC2

To provide a biochemical basis for our assignment of the ODC1 and ODC2 proteins as a monofunctional ODC and a bifunctional Lys/ODC, respectively, we purified each as 6His-Sumo-tagged proteins and tested their ability to decarboxylate Arg, Lys and Orn. Neither protein had detectable activity with Arg as substrate. With Orn, the 6His-Sumo-ODC1 had a specific activity of 4.1 U, but no activity with Lys as substrate. The 6His-Sumo-ODC2 had specific activities of 8.6 and 0.9 U using Orn and Lys, respectively, as substrates. These results match our prediction of the substrates decarboxylated by each enzyme [14].

ODC2 is the major enzyme for Put synthesis in *S. meliloti*

To determine the importance of ODC1 and ODC2 in PA synthesis, we constructed single and double mutants of strain Rm8530 in which the encoding gene(s) were inactivated (Table 1). Because both the *odc1* and *odc2* genes are present in operons [37], the inactivation of either gene probably also prevents the transcription of downstream gene(s) in the operons. For *odc1*, the downstream genes encode a Put transporter (PotE; SMa0678) and a ABC transporter substrate binding protein possibly for glutamate/aspartate (SMa0677). The products of these genes are probably not the only ones responsible for Put or glutamate/aspartate transport, since *S. meliloti* encodes an additional Put ABC transporter and three Spd/Put ABC transporters, in addition to numerous amino acid transport systems, both general and specific [14,26]. The single downstream gene (*smc02982*) in operon with *odc2* encodes a possible *N*-acetyltransferase that we proposed might function in the production of *N*-acetylglutamate for Orn and Arg biosynthesis [26, 41]. We found, however, that a *smc02982* null mutant of *S. meliloti* 1021 was an Arg prototroph that grew normally on MMS [41].

Cultures of the wild type and mutants were grown in MMS and their ability to decarboxylate Orn was determined. In comparison to the wild type, the ODC activities of the Rm8530 *odc1*, *odc2* and *odc1 odc2* mutants were decreased by 14, 55 and 75 %, respectively (Fig. 2). We conclude that it is much more likely that these reductions in ODC activity result from the inactivation of *odc1* and/or *odc2* rather than of downstream genes in their operons. From these results we estimate that all but about 25 % of the total ODC activity in strain Rm8530 is due to the combined activities of the ODC1 and ODC2, with the latter enzyme accounting for about 80 % of this. The remaining ODC activity in the double mutant could result from the predicted ADC (SMA0682) being able to decarboxylate Orn in addition to or instead of Arg, or by the conversion of the ^{14}C -Orn assay substrate to ^{14}C -Arg by enzymes of the Arg biosynthesis pathway [27], with subsequent decarboxylation of the ^{14}C -Arg by the ADC.

The wild type and mutant strains were grown in MMS under control (non-stress) or abiotic stress conditions to determine how inactivating the decarboxylases affected growth and PA production (Fig. 3). Estimations of relative changes in PA levels were made by densitometry of DNS-PA spots on HPTLC plates from at least two independent experiments. Specific growth rates (generations h^{-1}) for selected cultures are shown in Fig. 4. The growth of the mutant strains in PY rich medium was indistinguishable from that of the wild type (results not shown).

In wild type Rm8530 grown under control conditions, HSpd, Spd and Put account for virtually all of the DNS-PAs detected by HPTLC (Fig. 3(d)): relative to this total quantity set at 1.0, the proportions comprised by each of the three polyamines are 0.31, 0.56 and 0.13, respectively. During growth under the control, saline or acidic conditions, the *odc1* mutant grew similarly to the wild type (Fig. 3 (a) - (c)) and its content of HSpd, Spd and Put differed from the wild type by less than 10 %. In contrast, the *odc2* single and *odc1 odc2* double mutants grew about 40 % slower than the wild type or the *odc1* mutant (Fig. 4) and reached a lower cell yield under all conditions, most notably with acid stress (Fig. 3(a)-(c)). In the rhizobial plant

pathogen *Agrobacterium tumefaciens* strain C58, an *odc* deletion mutant produced much less Put and Spd and grew more slowly than the wild type in minimal medium [25]. The *A. tumefaciens* ODC and the *S. meliloti* ODC2 share over 90 % deduced amino acid sequence identity and may thus fulfill similar physiological functions.

In the wild type under saline stress (Fig. 3(d)), HSpd was undetectable and Put decreased by > 90 %, but Spd levels were maintained at a high level similar to that seen under control conditions. HSpd levels decrease in salt-stressed *Sinorhizobium fredii* P220 (a relatively salt- and acid-resistant strain), where it was proposed that having less of this polycation offsets the increase in positive charges caused by the rise in cytosolic K^+ that occurs under these conditions [18]. With acidic stress, wild type Rm8530 had a nearly 4-fold decrease in Put, while HSpd and Spd levels remained constant. In *S. fredii* P220 HSpd levels increase 2-fold at pH 4 as compared to pH 9.5, which is an acidic stress much more drastic than the pH 5.5 versus pH 6.8 stress that we imposed on *S. meliloti* in our experiments. Under acidic conditions, HSpd may provide cytosolic buffering or protect macromolecules from acid denaturation [18].

PA levels in the *odc1* mutant differed by no more than 10 % from the wild type under all of the growth conditions tested. The *odc2* mutant grown under control conditions lacked detectable Put and produced 9 and 18 % the wild type levels of HSpd and Spd, respectively. It also contained some apparent NSpd in the free fraction that accounted for 4.3 % of the total PAs. The PA profile of the *odc1 odc2* double mutant from control cultures was similar to that of the *odc2* single mutant (including the presence of free NSpd), except that Put was present at 11 % of the wild type level. The reduction in growth caused by the inactivation of the *S. meliloti odc2* is similar to what occurs in *R. leguminosarum* and *A. tumefaciens* when Put synthesis is lowered by treatment with the ODC inhibitor dimethylfluoroornithine or by inactivation of the *odc* gene, respectively [23,25]. In both the *odc2* and double

mutants, the levels of Put, Spd and HSpd were also markedly lower than in the wild type during growth under salt or acid stress (Fig. 3 (d)).

Chemical complementation restores growth and PA levels in the *odc2* mutant

Testing the ability of an exogenous PA to restore the normal phenotype of a PA mutant is called chemical complementation [9,11,23,24]. The effect of chemical complementation on the specific growth rate (μ , or generations h^{-1} ; Fig. 4) and PA content (Fig. 5) of the Rm8530 wild type and selected PA mutants was determined under control, salt stress and acid stress conditions. For these experiments, we used exogenous Put and Spd for chemical complementation since these PAs result directly or indirectly from Orn decarboxylation (Fig. 1). HSpd is derived directly from Put but was not tested because it is not commercially available. NSpd was used for chemical complementation since its synthesis does not require Put (Fig. 1).

In control (non-stressed) cultures without added PAs, μ values of the *odc1*, *odc2* and *odc1 odc2* mutants were 93, 59 and 60 % that of the wild type (Fig. 4(a)). The specific growth rate of the *odc1* mutant grown under stress or non-stress conditions with or without exogenous PAs differed from the wild type by no more than 13 %, in contrast to the much more pronounced growth defects found in the *odc2* and *odc1 odc2* mutants. As mentioned, the levels of Put, HSpd and Spd in the *odc1* mutant are comparable to those of the wild type, while they are similarly and drastically reduced to low levels in the *odc2* and double mutants (Fig. 3(d)). In cultures without added PAs, growth under salt and acidic stress reduced the μ of Rm8530 by 21 and 27 %, respectively, in comparison to non-stress conditions (Fig. 4). Under salt stress conditions, the μ values of the mutants were less affected relative to the wild type grown under the same condition, with the *odc1*, *odc2* and double mutants having 102, 86 and 85 % wild type growth rates (Fig. 4(b)). This may occur because *S. meliloti* responds to salt stress by lowering its total PA content (Fig. 3(d)), and so the *odc2* and double mutants, with their very low PA levels, are less affected for growth under saline conditions than under control conditions. Under acid stress, the *odc1*, *odc2* and double mutants had μ values of

105, 57 and 55 % of wild type (Fig. 4(c)). Thus, under this stress condition, the lack of ODC1 activity has essentially no effect on growth, while the mutants lacking ODC2 activity have growth reductions similar to that found under control conditions.

For wild type Rm8530 grown under control (non-stress) conditions (Fig. 4(a)), exogenous Put or Spd caused a reduction in μ of 8-9 % and NSpd caused a 21 % decrease. Lesser decreases in wild type μ values were caused by the PAs under salt stress (reductions of 4, 6 and 12 % for Put, Spd and NSpd, respectively). Under acid stress, wild type μ values decreased 7 % with Put, increased 1.1 fold with Spd and were unchanged with NSpd. For the *odc2* and double mutant grown under stress or non-stress conditions, Put supplementation restored μ to 94 to 96 % that of wild type. When these mutants were grown under control or salt stress conditions, exogenous Spd restored growth rates to 89-96 % that of wild type, while under acid stress it allowed growth at slightly higher than wild type μ values (Fig. 4). When grown in NSpd-supplemented cultures under non-stress conditions, the growth of the *odc2* and double mutants were restored to only 66 and 69 % that of wild type, respectively. Under salt and acid stress, these values ranged from 79-89 % of wild type. Thus, exogenous NSpd was not as effective as Put or Spd in restoring the growth of *odc2* and double mutants under any growth condition. It is interesting to note that the growth restoration caused with NSpd was greater under stress than non-stress conditions.

Under control conditions, Rm8530 cells from cultures grown with 1 mM Put (Fig. 5(a)) had 77 % less Put, 30 % less Spd and 1.9-fold more HSpd relative to cells grown without added Put (Fig. 3(d) and results not shown). Cells from the Put-supplemented cultures also contained a trace of DAP, which accounted for than 1 % of the total PAs present (Fig. 5(a)). The decrease in Put might result from its use in HSpd synthesis. DAP is not derived from Put and it is not known whether Put can modulate the production of PAs in the L-aspartate β -semialdehyde (L-Asp β -SA) branch of the synthesis pathway (Fig. 1).

Supplementation of Rm8530 control cultures with Spd caused a modest (13 %) decrease in intracellular Spd concentration, a 1.6-fold increase in Put and no change in HSpd, but caused the appearance of detectable DAP (Fig. 3(d) and Fig. 5(b) and results not shown). As described later, the drastic reduction in *odc2* transcription observed in cells from Spd-supplemented cultures suggests that the nearly unchanged level of intracellular Spd could result from its reduced synthesis by ODC2 being offset by the uptake of exogenous Spd. Whether the increase in Put is derived from the retroconversion of Spd to Put, as occurs in *A. tumefaciens* [11], is unknown. In Spd-supplemented MMS-salt cultures, HSpd was undetectable while Put and DAP levels were greatly decreased in comparison to their levels in the control cultures. Under these conditions, Spd was the only PA present at high levels. Cultures grown under acidic conditions with added Spd produced significantly less HSpd and Put than non-stressed cultures, but had the same or slightly higher levels of DAP. For all of the strains grown under all conditions, the addition of NSpd to the medium resulted in a high level of its accumulation, an apparent total absence of Spd and at most trace levels of HSpd and Put, and remarkably high amounts of DAP (Fig. 5(c)). In *A. tumefaciens*, cells grown in the presence of NSpd (which is not produced by this organism) also produce little intracellular Spd [25]. In *S. meliloti*, the intriguing possibility exists that NSpd has regulatory effects on the production on PAs derived from Put.

Genetic complementation restores growth and PA levels in the *odc2* mutant

To confirm that the inactivation of the *odc2* gene was responsible for the altered phenotype of the *odc2* mutant, we introduced the *odc2* gene into the mutant on plasmid pBB5-*odc2* (Table 1). The resulting transconjugant, 8530 *odc2*(pBB5-*odc2*), had its Orn decarboxylating activity restored to nearly that of the wild type, while the activity in the mutant containing the cloning vector alone (strain 8530 *odc2*(pBB5)) was very similar to that of the uncomplemented mutant (Fig. 2). Strain 8530 *odc2*(pBB5-*odc2*) also grew similarly to the wild type under stress and non-stress growth conditions, and its ability to produce PAs was restored to approximately wild type levels (Fig. 6). These results are consistent with the

inactivation of the *odc2* gene being the cause of the growth and PA production phenotypes of the *odc2* mutant. The *odc2* mutant also produced some apparent NSpd in the free PA fraction (Fig. 6(d)). In comparison to the uncomplemented mutant, strain 8530 *odc2*(pBB5) had a slower growth rate under all conditions, perhaps due to the metabolic burden of plasmid maintenance. As expected, strain 8530 *odc2*(pBB5) produced low levels of PAs similar to the mutant without the plasmid (Fig. 6).

Although the introduction of genes for metabolic enzymes cloned on plasmid pBB5 into *S. meliloti* can increase the gene products activity several-fold, presumably due to increased copy number [27], we did not find increased in ODC activity (Fig. 2) or over-production of PAs (Fig 6(d)) in strain 8530 *odc2*(pBB5-*odc2*).

Transcriptional expression of *odc2* under different growth conditions

The expression of β -glucuronidase (*gusA*) transcriptional fusions to the *odc1* and *odc2* genes was determined in strain Rm8530 grown under different growth conditions. The *odc1* gene is part of a predicted four gene operon and lacks a transcriptional start site (TSS) [37]: we found that a *odc1::gusA* fusion produced a low level of Gus activity (50-115 nmol min⁻¹ mg protein⁻¹). *In vivo*, *odc1* transcription may be linked to that of the upstream gene (*smc0682*), which is not part of the fusion construct.

Under the growth conditions tested, the GUS specific activity from the *odc2::gusA* fusion changed over a 7-fold range, from about 400 to 2900 nmol min⁻¹ mg protein⁻¹ (Fig. 7). Although *odc2* also lacks a recognizable TSS, it is the first gene in an apparent two-gene operon [37] and the results described below suggest that *odc2* expression is modulated in response to growth conditions.

In comparison to control (non-stress) conditions, *odc2* transcription decreased 69 % under salt stress (Fig. 7), consistent with the 94 % reduction in Put in these cells (Fig 3(d) and results not shown). The decreased Put content in salt stressed cells

is not explained by its conversion to HSpd and/or Spd, since the combined quantity of these PAs was nearly identical in the control and salt-stressed cells. Decreased expression of *odc2* was also reported in a transcriptomic study of *S. meliloti* 1021 grown under salt stress [42]. Acidic stress increased *odc2* transcription 1.5-fold, which does not correlate with the 77 % decrease in Put levels seen during growth at low pH (Fig. 3(d)).

Cells grown in cultures supplemented with the exogenous Put precursor amino acids Arg or Orn expressed *odc2* at a level 20 and 28 % less than in cells from unsupplemented cultures. Assigning these effects solely to the exogenous amino acid added to the cultures is complicated by the ability of *S. meliloti* to convert Arg to Orn using arginase and to metabolize Orn to Arg by activities of the Arg synthesis pathway [14]). We can tentatively conclude that Orn, the major substrate for ODC2, does not induce *odc2* expression.

To determine the effect of exogenous PAs on *odc2* transcription, we used Put and Spd, which result directly and indirectly from Orn decarboxylation, respectively, and DAP and NSpd, which are not derived from Put (Fig 1). Exogenous Put, Spd and NSpd inhibited *odc2* transcription by 58, 79 and 36 % respectively, while DAP resulted in a small increase in its transcription (Fig. 7). Thus, the PA products resulting from Orn decarboxylation inhibited *odc2* transcription to a greater degree than the PAs from the L-Asp β -SA branch of the pathway.

In summary, we have shown that Put and/or PAs derived from it are required for the normal growth of *S. meliloti* Rm8530. ODC2 (SMc02983) is a bifunctional Lys/Orn decarboxylase responsible for synthesizing the majority of Put produced by strain Rm8530, and changes in *odc2* transcription observed under some growth conditions are consistent with observed changes in PA levels. The *S. meliloti* ODC1 (SMa0680) is a monofunctional ODC that contributes a minor portion of the ODC activity in Rm8530.

The results presented here provide a basis for further experiments aimed at deciphering the enzymology and regulation of PA metabolism in *S. meliloti*, which provides an attractive model system due to its extended PA biosynthetic capabilities [14]. We are currently addressing some of these questions, along with determining the physiological roles of specific PAs in free-living and symbiotically-associated *S. meliloti*.

Funding information

Work at the UNAM was supported by DGAPA-PAPIIT Grants IN210114 and IN206317 to M. F. D. The York Centre of Excellence in Mass Spectrometry was created thanks to a major capital investment through Science City York, supported by Yorkshire Forward with funds from the Northern Way Initiative, and subsequent support from EPSRC (EP/K039660/1; EP/M028127/1).

Acknowledgements

Victor A. Becerra-Rivera is a doctoral student from Programa de Doctorado en Ciencias Biomédicas, Universidad Nacional Autónoma de México (UNAM) and received fellowship 574042 from CONACYT. We thank María J. Soto (Departamento de Microbiología del Suelo y Sistemas Simbióticos de la Estación Experimental del Zaidín, CSIC, Granada, Spain) for providing *S. meliloti* strain Rm8530 and Lourdes Girard (CCG-UNAM) for providing the p53lw primer and the pBBRMCre plasmid.

Conflict of interest

The authors declare that there are no conflicts of interest.

References

1. Tabor CW, Tabor H. Polyamines. *Annu Rev Biochem* 1984;53:749-790.
2. Hamana K, Matsuzaki S. Polyamines as a chemotaxonomic marker in bacterial systematics. *Crit Rev Microbiol* 1992;18:261-283.

3. Algranati ID. Polyamine metabolism in *Trypanosoma cruzi*: studies on the expression and regulation of heterologous genes involved in polyamine biosynthesis. *Amino Acids* 2010;38:645-51.
4. Miller-Fleming L, Olin-Sandoval V, Campbell K, Ralser M. Remaining mysteries of molecular biology: The role of polyamines in the cell. *J Mol Biol* 2015;427:3389–3406.
5. Michael AJ. Polyamines in eukaryotes, bacteria, and archaea. *J Biol Chem* 2016;291:14896-14903.
6. Soksawatmaekhin W, Kuraishi A, Sakata K, Kashiwagi K, Igarashi K, Excretion and uptake of cadaverine by CadB and its physiological functions in *Escherichia coli*. *Mol Microbiol* 2004;51:1401–1412.
7. Sturgill G, Rather PN. Evidence that putrescine acts as an extracellular signal required for swarming in *Proteus mirabilis*. *Mol Microbiol* 2004;51:437-446.
8. Shah P, Swiatlo E. A multifaceted role for polyamines in bacterial pathogens. *Mol Microbiol* 2008;68:4–16.
9. Lee J, Sperandio V, Frantz DE, Longgood J, Camilli A *et al.* An alternative polyamine biosynthetic pathway is widespread in bacteria and essential for biofilm formation in *Vibrio cholerae*. *J Biol Chem* 2009;284:9899-907.
10. Cockerell SR, Rutkovsky AC, Zayner JP, Cooper RE, Porter LR *et al.* *Vibrio cholerae* NspS, a homologue of ABC-type periplasmic solute binding proteins, facilitates transduction of polyamine signals independent of their transport. *Microbiology* 2014;160:832-843.
11. Kim SH, Wang Y, Khomutov M, Khomutov A, Fuqua C, Michael AJ. The essential role of spermidine in growth of *Agrobacterium tumefaciens* is determined by the 1,3-diaminopropane moiety. *ACS Chem Biol* 2016;11:491-9.
12. López-Gómez M, Hidalgo-Castellanos J, Lluch C, Herrera-Cervera JA. Epibrassinolide ameliorates salt stress effects in the symbiosis *Medicago truncatula*-*Sinorhizobium meliloti* and regulates the nodulation in cross-talk with polyamines. *Plant Physiol Biochem* 2016;108:212-221.

13. Lucas PM. Ornithine and lysine decarboxylation in bacteria. In: D'Mello FJ (editor) *Handbook of Microbial Metabolism of Amino Acids*. Wallingford, Oxfordshire: CAB International; 2017. pp. 116-127.
14. Dunn MF. Rhizobial Amino Acid Metabolism: Polyamine Biosynthesis and Functions. In: D'Mello FJ (editor) *Handbook of Microbial Metabolism of Amino Acids*. Wallingford, Oxfordshire: CAB International; 2017. pp. 352-370.
15. Hamana K, Minamisawa K, Matsuzaki S. Polyamines in *Rhizobium*, *Bradyrhizobium*, *Azorhizobium* and *Agrobacterium*. *FEMS Microbiol Lett* 1990;71: 71-76.
16. Hamana K, Sakamoto A, Tachiyanagi S, Terauchi E, Takeuchi M. Polyamine profiles of some members of the alpha subclass of the class Proteobacteria: Polyamine analysis of twenty recently described genera. *Microbiol Cult Coll* 2003;19:13-21.
17. Vassileva V, Ignatov, G. Polyamine-induced changes in symbiotic parameters of the *Galega orientalis-Rhizobium galegae* nitrogen-fixing system. *Plant Soil* 1999;210:83-91.
18. Fujihara S, Yoneyama T. Effects of pH and osmotic stress on cellular polyamine contents in the soybean rhizobia *Rhizobium fredii* P220 and *Bradyrhizobium japonicum* A1017. *Appl Environ Microbiol* 1993;59:1104-1109.
19. López-Gómez M, Hidalgo-Castellanos J, Iribarne C, Lluch C. Proline accumulation has prevalence over polyamines in nodules of *Medicago sativa* in symbiosis with *Sinorhizobium meliloti* during the initial response to salinity. *Plant Soil* 2014;374: 149-159.
20. Palma F, López-Gómez M, Tejera NA, Lluch C. Involvement of abscisic acid in the response of *Medicago sativa* plants in symbiosis with *Sinorhizobium meliloti* to salinity. *Plant Sci* 2014;223:16-24.
21. López-Gómez M, Hidalgo-Castellanos J, Muñoz-Sánchez JR, Marín-Peña AJ, Lluch C, Herrera-Cerver, JA. Polyamines contribute to salinity tolerance in

- the symbiosis *Medicago truncatula*-*Sinorhizobium meliloti* by preventing oxidative damage. *Plant Physiol Biochem* 2017;116:9-17.
22. Braeken K, Daniels R, Vos K, Fauvart M, Debkumari Bachaspatimayum D, Vanderleyden J, Michiels J. Genetic determinants of swarming in *Rhizobium etli*. *Microbial Ecol* 2008;55:54-64.
23. Shaw FL. *From prediction to function: Polyamine biosynthesis and formate metabolism in the α - and ϵ -Proteobacteria*. Ph.D Thesis. England: Institute of Food Research, Norwich Research Park; 2011.
24. López-Gómez M, Cobos-Porras L, Prell J, Lluch C. Homospermidine synthase contributes to salt tolerance in free-living *Rhizobium tropici* and in symbiosis with *Phaseolus vulgaris*. *Plant Soil* 2016;404:413–425.
25. Wang Y, Kim SH, Natarajan R, Heindl JE, Brugerem EL *et al*. Spermidine inversely influences surface interactions and planktonic growth in *Agrobacterium tumefaciens*. *J Bacteriol* 2016;198:2682-2691.
26. Dunn MF. Key roles of microsymbiont amino acid metabolism in rhizobia-legume interactions. *Crit Rev Microbiol* 2015;41:411-451.
27. Hernández VM, Girard L, Hernández-Lucas I, Vázquez A, Ortiz-Ortiz C *et al*. Genetic and biochemical characterization of arginine biosynthesis in *Sinorhizobium meliloti* 1021. *Microbiology* 2015;161:1671-1682.
28. Dunn MF, Araíza G, Cevallos MA, Mora J. Regulation of pyruvate carboxylase in *Rhizobium etli*. *FEMS Microbiol Lett* 1997;157:301-306.
29. Sambrook J, Fritsch EF, Maniatis T. *Molecular Cloning: A Laboratory Manual* New York: Cold Spring Harbor Laboratory Press; 1989.
30. Landeta C, Dávalos A, Cevallos MA, Geiger O, Brom S, Romero D. Plasmids with a chromosome-like role in Rhizobia. *J Bacteriol* 2011;193:1317-1326.
31. Romano A, Trip H, Lolkema JS, Lucas PM. Three-component lysine/ornithine decarboxylation system in *Lactobacillus saerimneri* 30a. *J Bacteriol* 2013;195:1248-1254.
32. Girard L, Brom S, Dávalos A, López O, Soberón M, Romero, D. Differential regulation of *fixN*-reiterated genes in *Rhizobium etli* by a novel *fixL*-*fixK* cascade. *Mol Plant-Microbe Interact* 2000;13:1283-1292.

33. Goldschmidt MC, Lockhart BM. Rapid methods for determining decarboxylase activity: arginine decarboxylase. *Appl Microbiol* 1971;22:350-357.
34. Ngo TT, Brillhart KL, Davis RH, Wong RC, Bovaird JH *et al.* Spectrophotometric assay for ornithine decarboxylase. *Anal Biochem* 1987;160:290-293.
35. Phan APH, Ngo TT, Lenhoff HM. Spectrophotometric assay for lysine decarboxylase. *Anal Biochem* 1982;120:193-197.
36. Bradford MM. A rapid and sensitive method for the quantitation of microgram quantities of protein utilizing the principle of protein-dye binding. *Anal Biochem* 1976;72:248-254.
37. Schlüter JP, Reinkensmeier J, Barnett MJ, Lang C, Krol E, Giegerich R, *et al.* Global mapping of transcription start sites and promoter motifs in the symbiotic α -proteobacterium *Sinorhizobium meliloti* 1021. *BMC Genomics* 2013;14:156.
38. Slocum RD, Flores HE, Galston AW, Weinstein LH. Improved method for HPLC analysis of polyamines, agmatine and aromatic monoamines in plant tissue. *Plant Physiol* 1989;89:512-517.
39. Pedrol N, Tiburcio AF. Polyamines determination by TLC and HPLC. In: Roger MJR (editor). *Handbook of Plant Ecophysiology Techniques*. The Netherlands: Kluwer Academic Publishers; 2001. pp. 335–363.
40. Pellock BJ, Teplitski M, Boinay RP, Bauer WD, Walker GC. A LuxR homolog controls production of symbiotically active extracellular polysaccharide II by *Sinorhizobium meliloti*. *J Bacteriol* 2002;184:5067-5076.
41. Paulino, EM. Búsqueda del gen que codifica para la enzima *N*-acetilglutamato sintasa por mutagénesis. Bachelors Thesis. Mexico: Universidad Autónoma del Estado de Morelos; 2013.
42. Domínguez-Ferreras A, Pérez-Arnedo R, Becker A, Olivares J, Soto MJ, Sanjuán J. Transcriptome profiling reveals the importance of plasmid pSymB for osmoadaptation of *Sinorhizobium meliloti*. *J Bacteriol* 2006;188:7617-7625.

- 739 43. Kovach ME, Elzer PH, Hill DS, Robertson GT, Farris MA *et al.* Four new
740 derivatives of the broad-host-range cloning vector pBBR1MCS, carrying
741 different antibiotic-resistance cassettes. *Gene* 1995;160:175-176.
- 742 44. Schäfer A, Tauch A, Jäger W, Kalinowski J, Thierbach G, Pühler A. Small
743 mobilizable multi-purpose cloning vectors derived from the *Escherichia coli*
744 plasmids pK18 and pK19: selection of defined deletions in the chromosome
745 of *Corynebacterium glutamicum*. *Gene* 1994;145:69-73.
- 746 45. Martínez-Salazar JM, Romero D. Role of *ruvB* gene in homologous
747 recombination in *Rhizobium etli*. *Gene* 2000;243:125-131.
- 748 46. Figurski DH, Helinski DR. Replication of an origin-containing derivative of
749 plasmid RK2 dependent on a plasmid function provided in trans. *Proc Natl*
750 *Acad Sci (USA)* 1979;76:1648-1652.

Table 1. Strains and plasmids used in this study.

Strain or plasmid	Relevant characteristics	Source or reference
<i>E. coli</i> strains		
BL21(DE3)	Strain for protein expression	Invitrogen
DH5 α	Cloning strain	Laboratory collection
JM109	Cloning strain	Laboratory collection
<i>S. meliloti</i> strains		
Rm8530	<i>S. meliloti</i> 1021 <i>expR</i> ⁺ , Sm ^r	M. Soto, Estación Experimental del Zaidín, CSIC, Granada, Spain
8530 <i>odc1</i>	Rm8530 <i>sma0680::loxP</i> Sp <i>odc1</i> null mutant, Sm ^r Sp ^r	This study
8530 <i>odc2</i>	Rm8530 <i>smc02983::loxP</i> Sp <i>odc2</i> null mutant, Sm ^r Sp ^r	This study
8530 <i>odc1 odc2</i>	Rm8530 <i>sma0680::loxP smc02983::loxP</i> Sp <i>odc1 odc2</i> null double mutant, Sm ^r Sp ^r	This study
8530 <i>odc2</i> (pBB5)	Rm8530 <i>smc02983::loxP</i> Sp <i>odc2</i> null mutant containing plasmid pBB5, Sm ^r Sp ^r Gm ^r	This study
8530 <i>odc2</i> (pBB5- <i>odc2</i>)	Rm8530 <i>smc02983::loxP</i> Sp <i>odc2</i> null mutant complemented with the <i>odc2</i> gene <i>in trans</i> , Sm ^r Sp ^r Gm ^r	This study
Plasmids		
pBB5	Broad-host-range vector pBBR1MCS-5, Gm ^r	[43]
pBB5- <i>odc2</i>	pBBR1MCS-5 containing <i>smc02983</i> with native promoter and terminator regions, Gm ^r	This study
pBBMCS-53	Δ <i>placZ</i> pBBR1MCS-5 derivative	[32]

	with promoterless <i>gusA</i> , Gm ^r	
pBB53odc1:: <i>gusA</i>	Transcriptional <i>sma0680</i> :: <i>gusA</i> fusion in pBBMCS-53	This study
pBB53odc2:: <i>gusA</i>	Transcriptional <i>smc02983</i> :: <i>gusA</i> fusion in pBBMCS-53	This study
pCRodc1	Rm8530 genome region containing <i>odc1</i> cloned in pTopo	This study
pCRodc2	Rm8530 genome region containing <i>odc2</i> cloned in pTopo	This study
pKodc1	Rm8530 genome region containing <i>odc1</i> cloned in pK18mobsacB	This study
pKodc2	Rm8530 genome region containing <i>odc2</i> cloned in pK18mobsacB	This study
pK18mobsacB	Broad-host range gene replacement vector, Km ^r	[44]
pKodc1:: <i>loxSp</i>	<i>odc1</i> :: <i>loxP</i> Sp fragment cloned in pK18mobsacB	This study
pKodc2:: <i>loxSp</i>	<i>odc2</i> :: <i>loxP</i> Sp fragment cloned in pK18mobsacB	This study
pMS102 <i>loxSp</i> 17	Source of the <i>loxP</i> Sp interposon, Sp ^r	[45]
pRK2013	Helper plasmid, Km ^r	[46]
pET-Sumo	Expression vector for production of 6His-Sumo-tagged proteins, Km ^r	Invitrogen
pSumo-odc1	pET-Sumo containing the cloned Rm8530 <i>odc1</i> gene	This study
pSumo-odc2	pET-Sumo containing the cloned Rm8530 <i>odc2</i> gene	This study
pTopo	pCR2.1Topo vector for cloning PCR products, Km ^r	Invitrogen
pTZ57R/T	InstAclone vector for cloning PCR	Thermo

products, Ap^r (Cb^r)

pBBRMCre

Plasmid used for deleting the loxP [30]

Sp interposon inserted in *smc0680*

760

761

762

763

FIGURE LEGENDS

Fig. 1. Predicted polyamine synthesis pathways in *S. meliloti* Rm8530. Abbreviations not described in the text: α -KG, α -ketoglutarate; CNSpd, carboxynorspermidine; CANSDC, CNSpd decarboxylase; CANSDH, CNSpd dehydrogenase; CSpd; carboxyspermidine; DABA, diaminobutyric acid; DABA AT, DABA aminotransferase; DABA DC, DABA decarboxylase; L-Glu, L-glutamate; HSS, homospermidine synthase. Modified from [14].

Fig. 2. Specific activities of Orn decarboxylation by *S. meliloti* strains grown in MMS, normalized to that of the Rm8530 wild type (100 % = 3968 U). Values are the mean \pm SD for two independent experiments. Values for columns marked with the same letter are not statistically different according to a t-student test.

Fig. 3. Growth and PA content of *S. meliloti* cultured under non-stress and stress conditions. Panels (a), (b) and (c) represent culture growth under control, salt stress and acidic stress conditions, respectively. Strains and line colors: Rm8530 wild type, black; 8530 *odc1*, pink; 8530 *odc2*, green; 8530 *odc1 odc2*, blue. Panel (d) shows HPTLC detection of dansyl-PAs from 32 h cultures. Lane S contains dansyl-PA standards with their identities shown at the right side of the first plate image. *S. meliloti* dansyl-PA samples are: Lane 1, Rm8530; Lane 2, 8530 *odc1*; Lane 3, 8530 *odc2*; Lane 4, 8530 *odc1 odc2*.

Fig 4. Specific growth rates (μ , generations h^{-1}) of selected *S. meliloti* strains grown in MMS with or without chemical complementation with exogenous PAs. Panel (a), control conditions; panel (b), MMS-salt; panel (c), MMS-acid. The PA added to the cultures is indicated at the bottom of the figure. Bar colors represent: Rm8530 wild type, blue; 8530 *odc1*, orange; 8530 *odc2*, grey; 8530 *odc1 odc2*, yellow. Values are normalized to μ values of the wild type grown under the three conditions in media lacking added PAs, where 100 % corresponds to μ values of

0.179, 0.141 and 0.130 for the MMS, MMS-salt and MMS-acid cultures. Results are the mean \pm SD for 2 independent experiments.

Fig. 5. Effect of chemical complementation with exogenous PAs on PA production by *S. meliloti* strains. HPTLC detection of dansyl-PAs from 32 h cultures. Lane S contains dansyl-PA standards with their identities shown at the left side of the plates. Panel (a), MMS plus 1 mM Put; panel (b), MMS plus 1 mM Spd; panel (c), MMS plus 1 mM NSpd. Lane assignments for all plates: Lane 1, Rm8530 wild type; Lane 2, 8530 *odc1*; Lane 3, 8530 *odc2*; Lane 4, 8530 *odc1 odc2*.

Fig. 6. Growth and PA content of the genetically complemented 8530 *odc2* mutant. Panels (a), (b) and (c) show culture growth under control, salt stress and acidic stress conditions, respectively. Strains and line colors: Rm8530 wild type, black; 8530 *odc2*, green; 8530 *odc2*(pBB5-*odc2*), red; 8530 *odc2*(pBB5), purple. Panel (d) shows HPTLC detection of dansyl-PAs from 32 h cultures. Lane S contains dansyl-PA standards with their identities shown at the left side of the plate. *S. meliloti* dansyl-PA samples are: Lane 1, Rm8530; Lane 2, 8530 *odc2*; Lane 3, 8530 *odc2*(pBB5); Lane 4, 8530 *odc2*(pBB5-*odc2*).

Fig. 7. β -glucuronidase (Gus) activities produced by *S. meliloti* Rm8530 containing the *odc2::gusA* transcriptional fusion plasmid. Cells were grown in the indicated media for 16 h. Values are the mean \pm SD for two independent experiments, each with 2 technical replicates of two biological replicates. 1 U = nmol product min⁻¹ mg protein⁻¹.

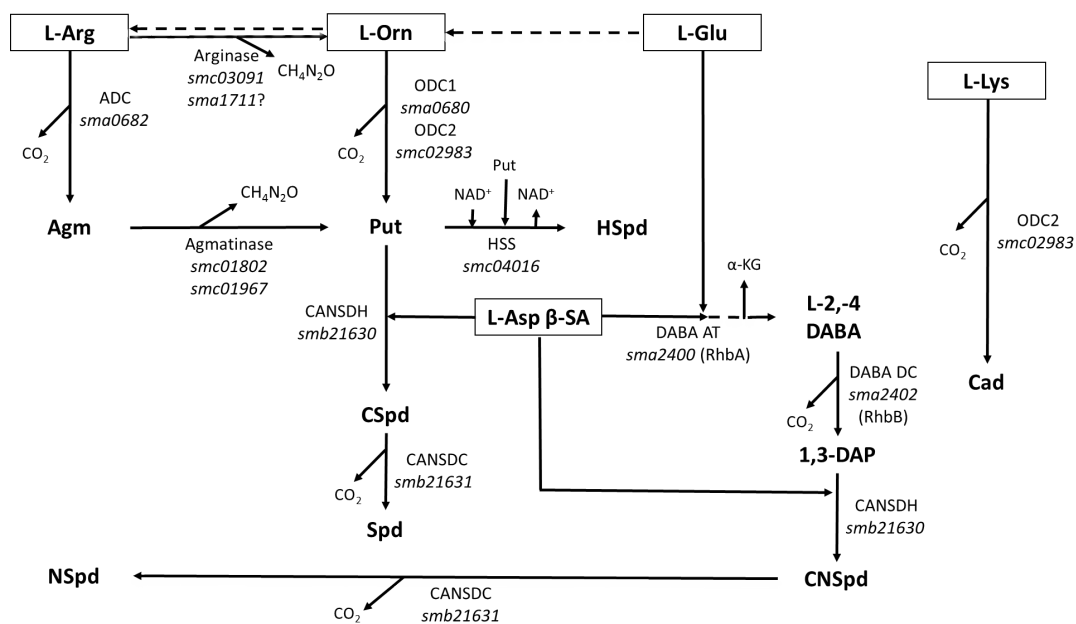


Fig. 1

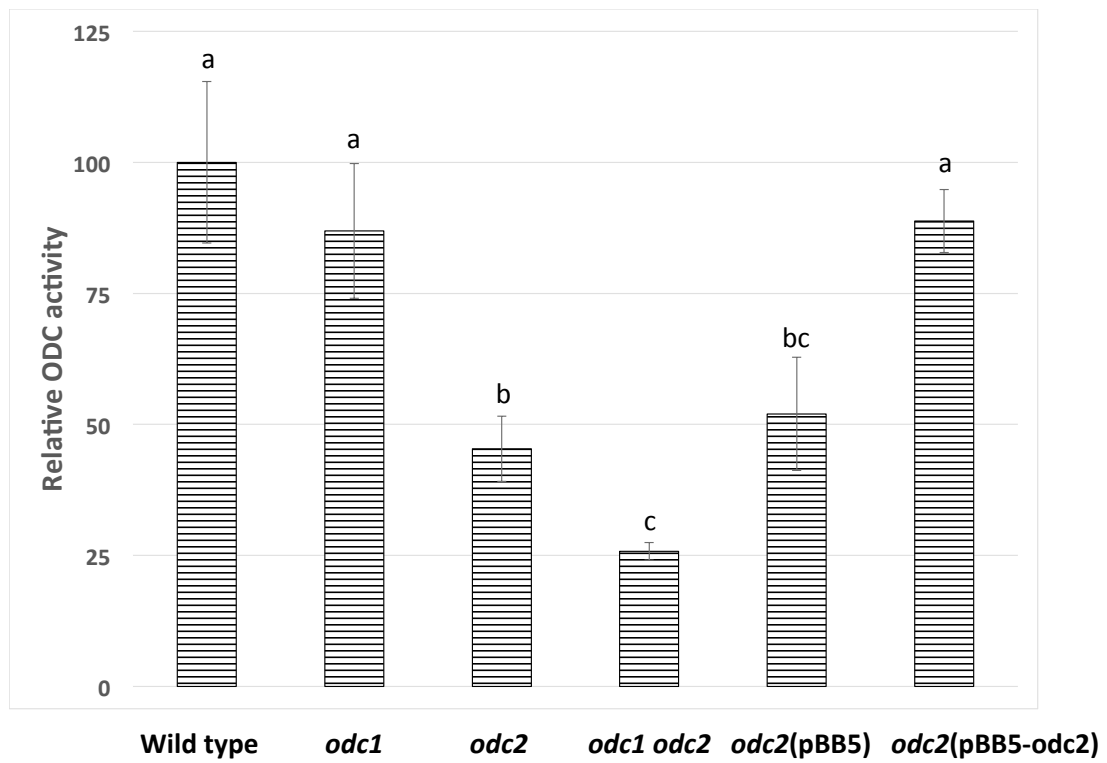


Fig. 2

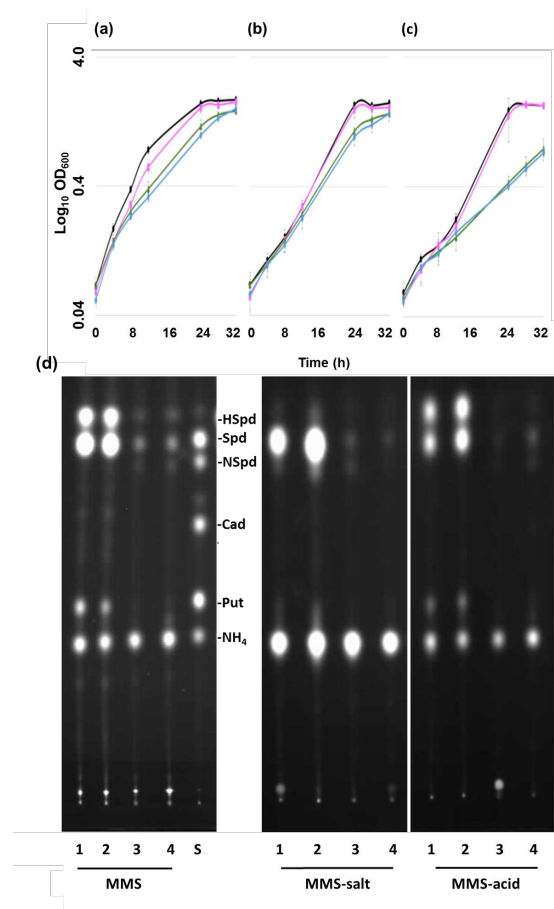
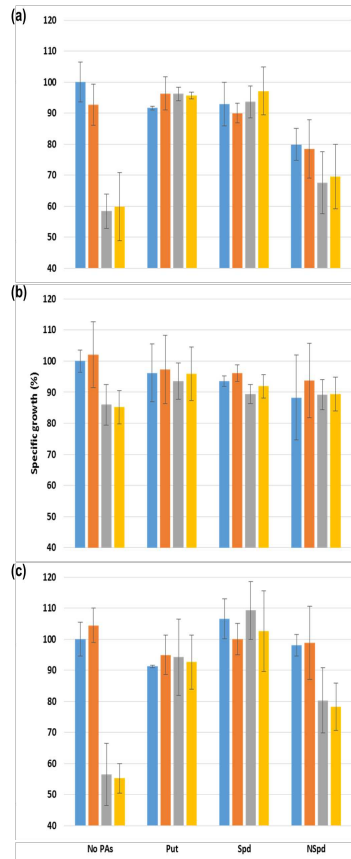


Fig. 3



835
836 Fig. 4

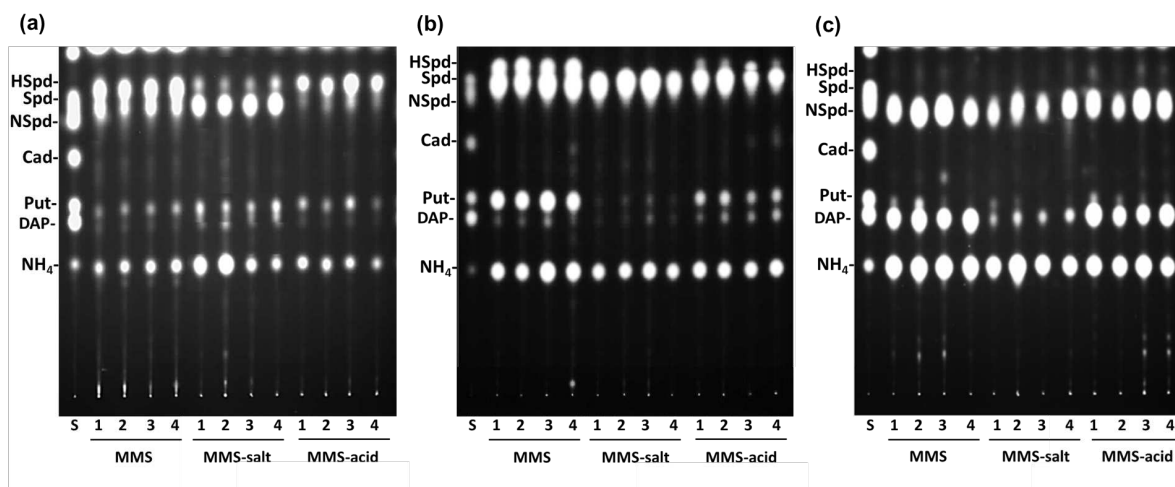


Fig. 5

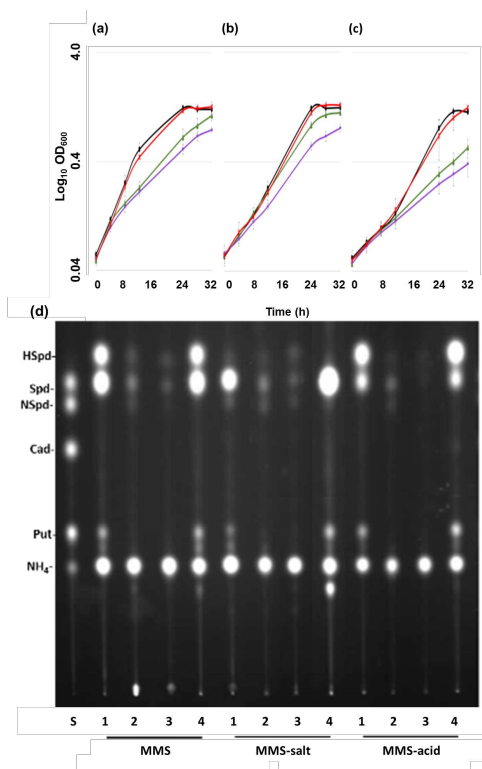


Fig. 6

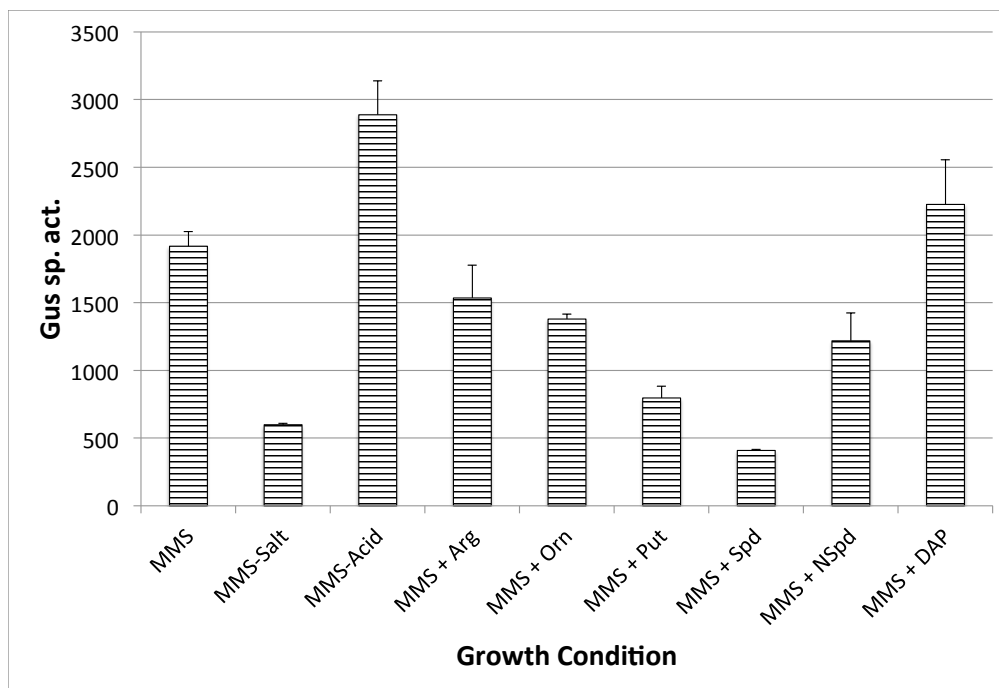


Fig. 7

Supplementary material

Table S1. Oligonucleotide primers used in this study.

Primer name	5'-3' nucleotide sequence	Description
Sumo0680F	GTGAAGGCTCCGACCGTC	Forward primer for amplifying the insert used in making pSumo-odc1 and pCR-odc1
Sumo0680R	GATTACTCGCGCACGGCG	Reverse primer for amplifying the insert used in making pSumo-odc1 and pCR-odc1
Sumo02983F	ATGGCCATGACCACCGC	Forward primer for amplifying the insert used in making pSumo-odc2
Sumo02983R	GGATCAGATGACATAGGCC	Reverse primer for amplifying the insert used in making pSumo-odc2
F-02983	TTG GCA CGC ACG AGATCG	Forward primer for amplifying the insert used in making pCR-odc2
R-02983	GGATCAGATGACATAGGCC	Reverse primer for amplifying the insert used in making pCR-odc2
0680gusF	CTACAACCGCCTGGTCAAG	Forward primer used in construction of pBB53odc1::gusA
0680gusR	TCCCAATATAGGCACCAACC	Reverse primer used in construction of pBB53odc1::gusA
02983gusF	GGATGCGGGTCAAGGTATC	Forward primer used in construction of pBB53odc2::gusA
02983gusR	TTGATGGTGTGCCATAGGA	Reverse primer used in construction of pBB53odc2::gusA
p53lw	ACAGGACGTAACATAAGGGAC T	Reverse primer for the <i>gusA</i> gene

Supplementary Material Figure Legend

Fig. S1. Analysis of PAs by mass spectrometry. As described in Methods, dansyl-PAs were prepared from authentic standards or isolated from *S. meliloti* cells, separated by HPTLC, eluted from the silica gel plates and characterized by matrix-assisted laser desorption/ionisation (MALDI) high resolution, high mass accuracy FT-ICR mass spectrometry (MS) and product ion tandem mass spectrometry (MS/MS). The fragmentation diagrams and product ion spectra used in the identification of the dansyl-PAs are presented in this figure. Panel (a), resolution by HPTLC of dansyl-PA standards and unknown bound (spots B1 and B2) or free (spots F1 through F3) PAs obtained from *S. meliloti* cells. Panel (b), structure of the dansyl (DNS) chemical group. Panel (c), fragmentation diagram of DNS-Put. Panel (d), product ion spectrum of DNS-Put standard. Standard Put (two amine groups, so acquires two DNS groups; Fig. S1(c)) gave an intense signal for its molecular species at m/z 555.20936 on MALDI FT-ICR mass spectrometry, corresponding to an elemental composition $C_{28}H_{35}N_4O_4S_2$ ($M+H^+$ for (dansyl)₂Put; 0.1 ppm mass error) and a pattern of isotopic signals matching in relative intensities very closely those predicted for this molecular composition. CID-MS-MS of the ion at m/z 555 yielded a product ion spectrum consistent with (dansyl)₂Put (Fig. S1(d)). The product ion at m/z 220 is related to that at m/z 234, by loss of one O atom with transfer of two H atoms. Component F1 migrated similarly to standard DNS-Put (Fig S1(a)). A strong signal was observed at m/z 555.20921 ($M+H^+$ for (DNS)₂Put; 0.4 ppm mass error), and the product ion spectrum is (Fig. S1(e)) indistinguishable from that obtained from the authentic standard DNS-Put (Fig. S1(d)), demonstrating that component F1 is Put. Panel (e), product ion spectrum of spot F1 (see panel (a)), identified as DNS-Put. Panel (f), fragmentation diagram of DNS-Spd. Panel (g), product ion spectrum of DNS-Spd standard. Standard Spd (adds three dansyl groups; Fig. S1(f)) gave an intense $M+H^+$ signal at m/z 845.31810 ($C_{43}H_{53}N_6O_6S_3$; 0.2 ppm mass error), and a pattern of isotopic signals that match very closely those predicted for a molecule with this composition. CID-MS-MS of the ion at m/z 845 yielded a product ion spectrum consistent with

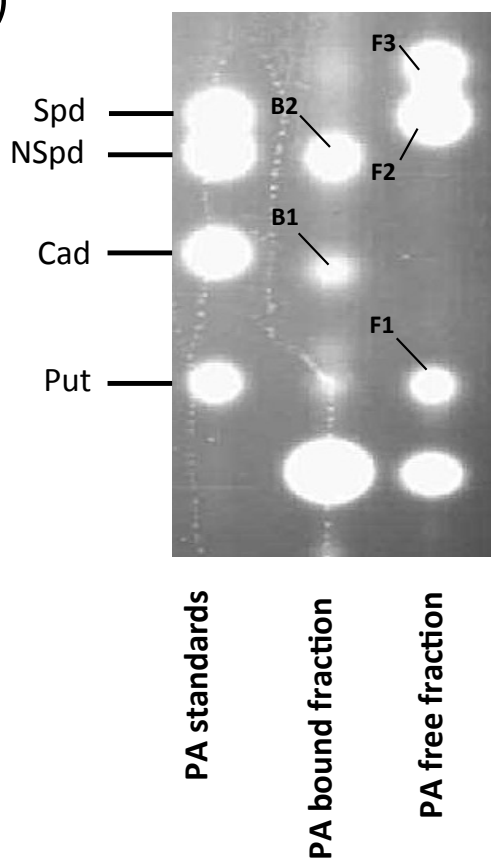
(dansyl)₃Spd (Fig. S1(g)). Component F2 migrated with the DNS-Spd standard (Fig. S1(a)). A very strong signal was observed at m/z 845.31794 ($M+H^+$ for (DNS)₃Spd; 0.5 ppm mass error), and the product ion spectrum (Fig. S1(h)) is very similar to that from standard DNS-Spd (Fig. S1(g)), identifying the component as DNS-Spd (Fig. S1(h)). Panel (h), product ion spectrum of spot F2 (see panel (a)), identified as DNS-Spd. Panel (i), fragmentation diagram of DNS-NSpd. Panel (j), product ion spectrum of DNS-NSpd standard. Standard NSpd (three dansyl groups; Fig. S1(i)) gave an intense $M+H^+$ signal at m/z 831.30233 ($C_{42}H_{51}N_6O_6S_3$; 0.4 ppm mass error), and a pattern of isotopic signals that match very closely those predicted for a molecule with this composition. CID-MS-MS of the ion at m/z 831 yielded a product ion spectrum consistent with (dansyl)₃NSpd (Fig. S1(j)). Panel (k), product ion spectrum of spot B2 (see panel (a)), identified as DNS-NSpd. Panel (l), fragmentation diagram of DNS-HSpd. Panel (m), product ion spectrum of spot F3 (see panel (a)), identified as DNS-HSpd. Component B2 gave a signal at m/z 831.30234 ($M+H^+$ for (DNS)₃NSpd; 0.4 ppm mass error) and a product ion spectrum that identifies this component as NSpd (Fig. S1(k)). Component F3 migrated above DNS-Spd (Fig. S1(a)) and did not correspond with any of the PAs for which authentic standards were available. Mass spectrometric analysis generated a strong signal at m/z 859.33357 consistent with $M+H^+$ for $C_{44}H_{55}N_6O_6S_3$, indicating a homologue of Spd with an additional CH_2 group (Fig. S1(l); 0.4 ppm mass error). The product ion spectrum (Fig. S1(m)) is consistent with (DNS₃)HSpd; note that the fragment ions at m/z 541 and 360 in the Spd spectrum are shifted to m/z 555 and 374 in that of HSpd, consistent with the presence of an additional backbone CH_2 group. The mass spectrum of a DNS-PA that migrated similarly to a DNS-Cad standard on HPTLC plates (Fig. S1(a), spot B1) gave an intense signal at m/z 569.22520 corresponding to an elemental composition $C_{29}H_{37}N_4O_4S_2$ ($M+H^+$ for (DNS)₂diaminopentane; 0.2 ppm mass error) and a pattern of isotopic signals matching in relative intensities very closely those predicted for this molecular composition. The product ion spectrum was not recorded, and so the substitution pattern was not determined. The identities of

918 DAP and NH_3 were assigned based only on their co-migration with DNS
919 derivatives of these compounds.

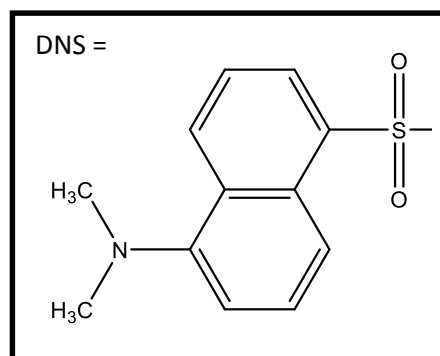
920

921

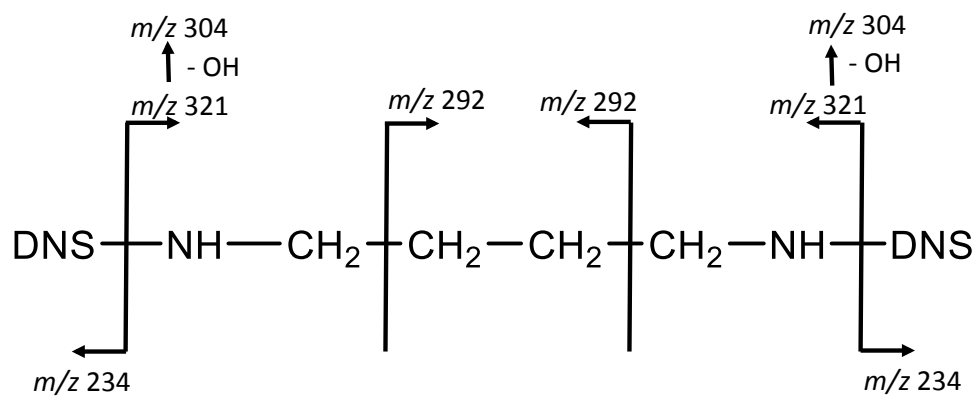
(a)



(b)

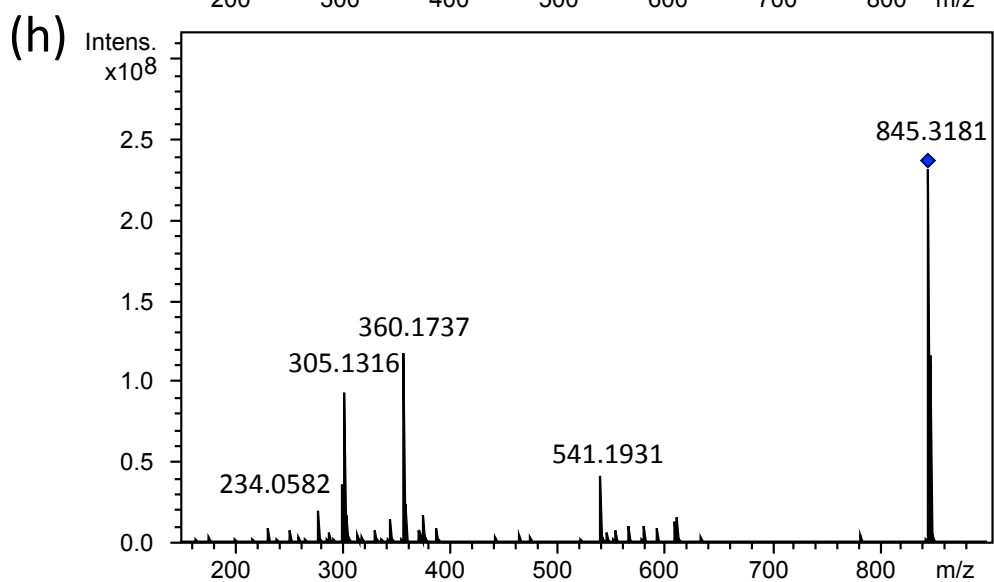
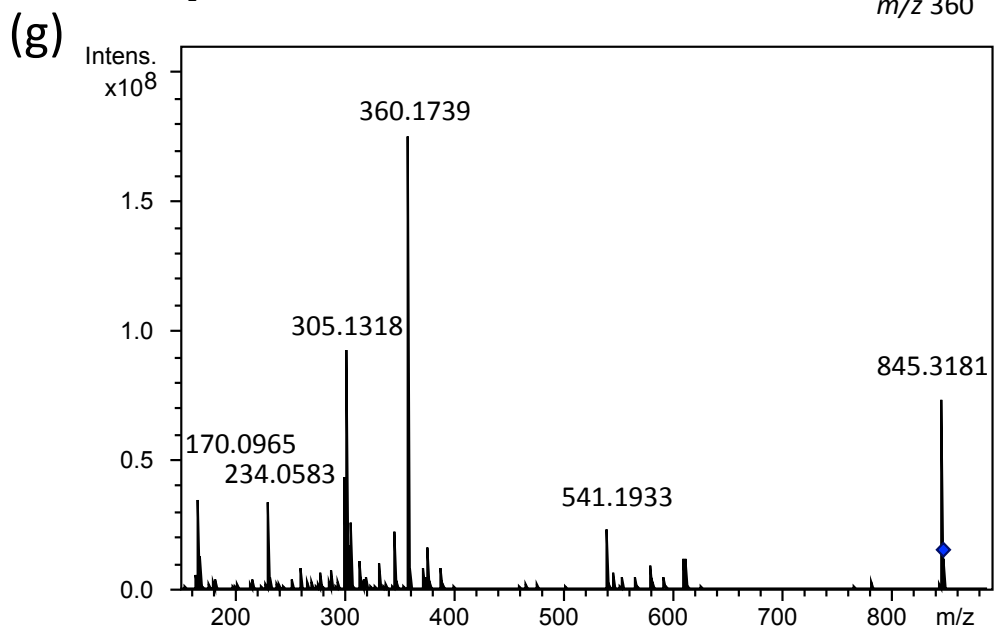
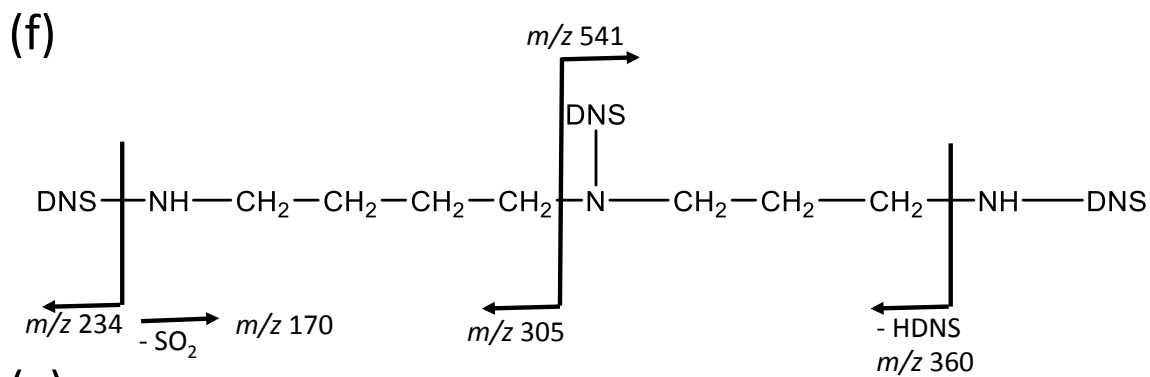


(c)



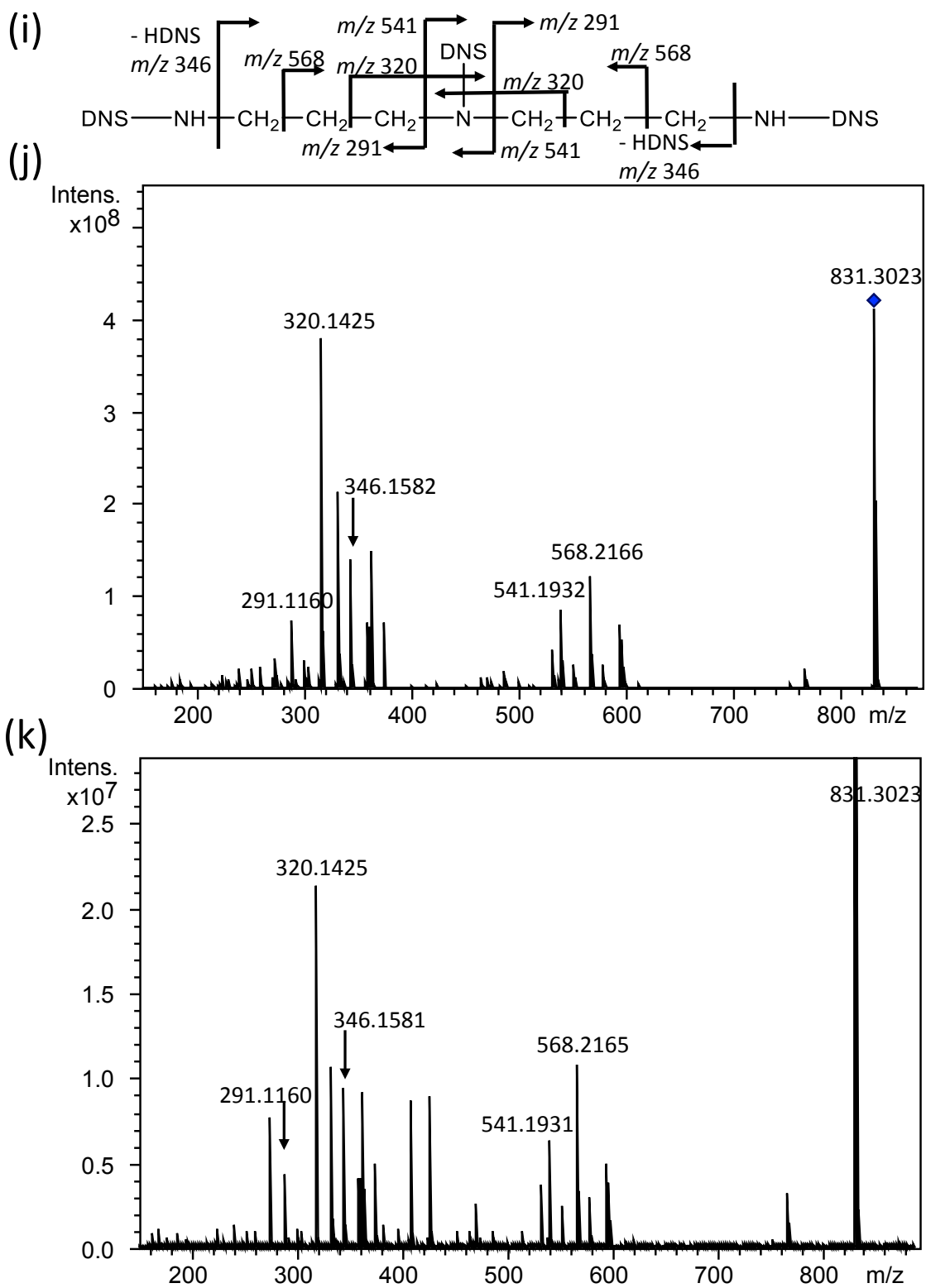
922

923



924

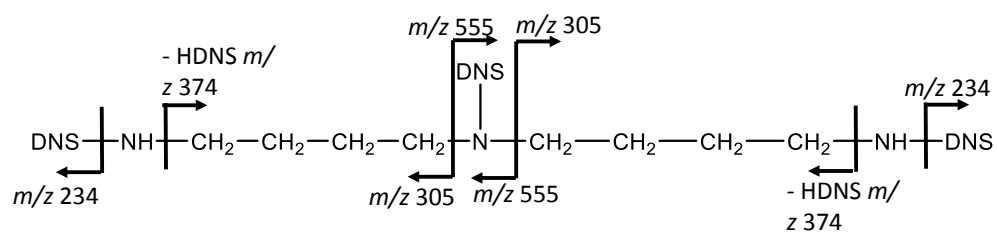
925



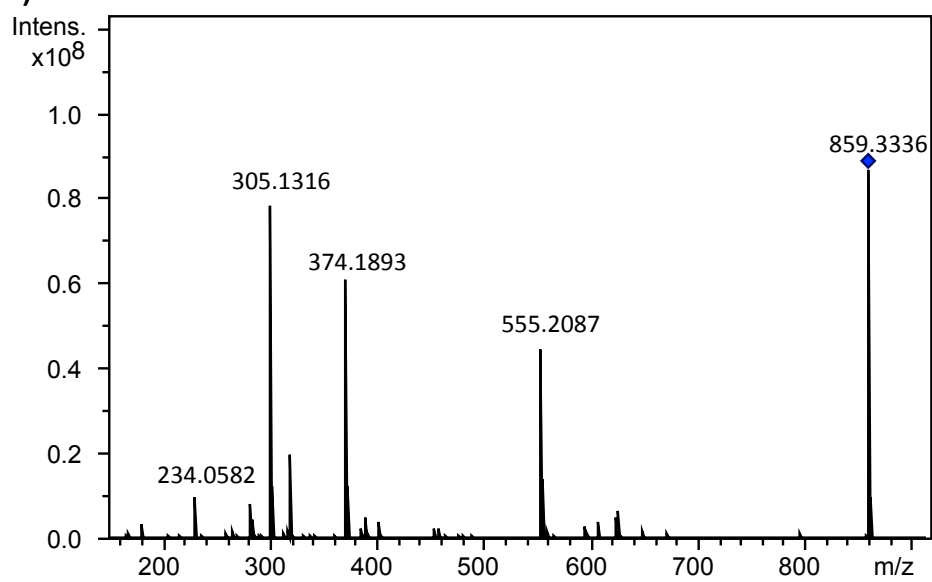
926

927

(1)



(m)



928

929 Fig. S1

930

931